

# Effects of dark energy on the efficiency of charged AdS black holes as heat engines

Hang Liu<sup>1,a</sup>, Xin-He Meng<sup>1,2,b</sup>

<sup>1</sup> School of Physics, Nankai University, Tianjin 300071, China

<sup>2</sup> State Key Laboratory of Theoretical Physics, Institute of Theoretical Physics, Chinese Academy of Science, Beijing 100190, China

Received: 18 May 2017 / Accepted: 6 August 2017 / Published online: 18 August 2017

© The Author(s) 2017. This article is an open access publication

**Abstract** In this paper, we study the heat engine where a charged AdS black hole surrounded by dark energy is the working substance and the mechanical work is done via the  $PdV$  term in the first law of black hole thermodynamics in the extended phase space. We first investigate the effects of a kind of dark energy (quintessence field in this paper) on the efficiency of the RN-AdS black holes as the heat engine defined as a rectangular closed path in the  $P$ - $V$  plane. We get the exact efficiency formula and find that the quintessence field can improve the heat engine efficiency, which will increase as the field density  $\rho_q$  grows. At some fixed parameters, we find that a larger volume difference between the smaller black holes ( $V_1$ ) and the bigger black holes ( $V_2$ ) will lead to a lower efficiency, while the bigger pressure difference  $P_1 - P_4$  will make the efficiency higher, but it is always smaller than 1 and will never be beyond the Carnot efficiency, which is the maximum value of the efficiency constrained by thermodynamics laws; this is consistent to the heat engine in traditional thermodynamics. After making some special choices for the thermodynamical quantities, we find that the increase of the electric charge  $Q$  and the normalization factor  $a$  can also promote the heat engine efficiency, which would infinitely approach the Carnot limit when  $Q$  or  $a$  goes to infinity.

## 1 Introduction

Since Hawking and Page [1] found that there exists a phase transition in the phase space between Schwarzschild-AdS black holes and thermal radiation (i.e. the Hawking-Page phase transition), much attention has been paid to the study of the thermodynamical properties of AdS black holes [2–25], especially to the study of AdS black hole thermodynamics in extended phase space in which the cosmological constant

$\Lambda$  is not only treated as the thermodynamical pressure  $P$  by the relation

$$P = -\frac{\Lambda}{8\pi} \quad (1.1)$$

but also a thermodynamical variable appearing in the first law of black hole thermodynamics such that the Smarr relation can be obtained. The  $P$ - $V$  criticality of RN-AdS black holes in extended phase space has been investigated by the authors in Ref. [2] with analogy between AdS black holes and van der Waals liquid-gas systems, the critical point and phase transition between large black hole and small black hole were discovered in this reference. Their study also showed that the electric charge  $Q$  plays a crucial role in the critical behavior of AdS black holes, and the charged AdS black holes, as a gravity system, is highly similar to van der Waals liquid-gas system from a thermodynamical perspective, and the two systems even have the same critical exponents. All of these discoveries suggest that the gravity system has a profound relation with the traditional thermodynamical system, while one used to think that these two systems do not have any relations.

Inspired by the progress in the understanding of black hole thermodynamics, one natural idea is to introduce the concept of a traditional heat engine into the black hole thermodynamics with both the thermodynamic pressure and volume defined in extended phase space. Johnson proposed this idea and firstly studied the charged AdS black holes as a heat engine defined by a closed path in the  $P$ - $V$  plane in Ref. [26] and calculated the efficiency of such a heat engine. This amazing proposal implies that the useful mechanical work of both static and stationary AdS black holes can be extracted from the heat energy, while the Penrose Process can only be used to extract energy from rotating black holes, but the Penrose process can be performed on black holes in both asymptotically AdS and flat spacetime. Moreover, it is

<sup>a</sup> e-mail: [hangliu@mail.nankai.edu.cn](mailto:hangliu@mail.nankai.edu.cn)

<sup>b</sup> e-mail: [xhm@nankai.edu.cn](mailto:xhm@nankai.edu.cn)

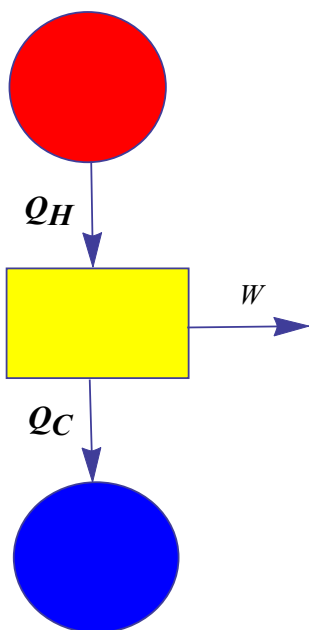


Fig. 1 The heat engine flows

argued that such a heat engine may have interesting holographic implications, because the engine cycle represents a course through a family of holographically dual large  $\mathcal{N}$  field theories [26]. Johnson’s pioneering work has drawn a lot of attention and has been generalized to many other black hole cases [27–41].

We would like to briefly introduce Johnson’s work [26] in the following context. Figure 1 represents the heat flows of the heat engine.  $Q_H$  represents the amount of the input heat and  $Q_C$  stands for the amount of exhaust heat; the work done by the heat engine is denoted  $W$ . Obviously, the heat engine efficiency can be computed as

$$\eta = \frac{W}{Q_H} = \frac{Q_H - Q_C}{Q_H} = 1 - \frac{Q_C}{Q_H}. \tag{1.2}$$

For the Carnot engine, the efficiency is

$$\eta_c = 1 - \frac{Q_C}{Q_H} = 1 - \frac{T_C}{T_H} \tag{1.3}$$

where  $T_C$  is the lower temperature and  $T_H$  is the higher temperature of the two heat sources, which make the heat engine work. It is clear that the efficiency of the Carnot engine is only dependent on the two temperatures of the heat sources. In Fig. 2, we give a kind of heat cycle of the heat engine of a static black hole and we show that this heat engine obeys the same efficiency formula as the Carnot heat engine. Along the upper isotherm ( $1 \rightarrow 2$ ) of Fig. 2, the amount of input heat is

$$Q_H = T_H \Delta S_{1 \rightarrow 2} = T_H \left( \frac{3}{4\pi} \right)^{\frac{2}{3}} \pi (V_2^{\frac{2}{3}} - V_1^{\frac{2}{3}}), \tag{1.4}$$

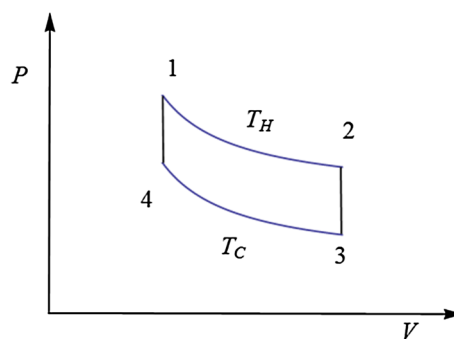


Fig. 2 Carnot engine

and along the lower isotherm ( $3 \rightarrow 4$ ) we get  $Q_C$ :

$$Q_C = T_C \Delta S_{3 \rightarrow 4} = T_C \left( \frac{3}{4\pi} \right)^{\frac{2}{3}} \pi (V_3^{\frac{2}{3}} - V_4^{\frac{2}{3}}). \tag{1.5}$$

Note that we have  $V_2 = V_3, V_1 = V_4$ , which yields

$$\eta_c = 1 - \frac{Q_C}{Q_H} = 1 - \frac{T_C}{T_H}, \tag{1.6}$$

which is exactly the Carnot engine heat efficiency in Eq. (1.3). The kernel of the calculations carried out above is that the black hole entropy and thermodynamic volume are not independent and they both are a function of the black hole horizon radius  $r_h$  such that the adiabats coincide with isochores. It is worth noting that the example calculation presented above holds for all the static AdS black holes; in this sense, this calculation is a general consideration for the calculation of the efficiency of heat engines generated by static AdS black holes.

Following the discussion above, we give an example [26] of the efficiency calculations of RN-AdS black holes as heat engines defined in Fig. 3 where the closed trajectory ( $1 \rightarrow 2 \rightarrow 3 \rightarrow 4 \rightarrow 1$ ) is a rectangle, so that it is very easy to calculate the work (i.e. the area of the rectangle) done by the heat engine. The Hawking temperature on the event horizon of RN-AdS black holes is

$$T = \frac{3r_+^4 + l^2 r_+^2 - q^2 l^2}{4\pi l^2 r_+^3}; \tag{1.7}$$

the cosmological radius  $\ell$  is related to the cosmological constant in four-dimensional spacetime by the relation  $\Lambda = -3/\ell^2$ . The pressure  $P$  can be expressed as

$$P = \frac{1}{8\pi} \left( \frac{4\pi}{3} \right)^{\frac{4}{3}} \left( \frac{3T}{V^{\frac{1}{3}}} - \left( \frac{3}{4\pi} \right)^{\frac{2}{3}} \frac{1}{V^{\frac{2}{3}}} + \frac{q^2}{V^{\frac{4}{3}}} \right), \tag{1.8}$$

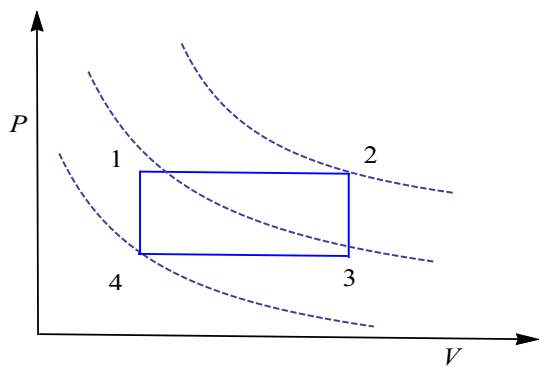


**Fig. 3** The engine mainly discussed in this paper. Dashed lines represent the isothermals

the heat capacity is

$$C = T \frac{\partial S}{\partial T} = \left(1 - \frac{2S}{\sqrt{\pi}} \frac{\partial P}{\partial T}\right) 2S \left(\frac{8PS^2 + S - \pi q^2}{8PS^2 - S + 3\pi q^2}\right) \tag{1.9}$$

where  $S$  represents the black hole entropy. The heat capacity  $C_P$  under constant pressure can be obtained by the condition  $\partial P/\partial T = 0$ . Note that we have

$$\left(\frac{\partial P}{\partial T}\right)_V = \frac{\sqrt{\pi}}{2\sqrt{S}}, \tag{1.10}$$

and we substitute Eq. (1.10) into Eq. (1.9) to calculate the heat capacity  $C_V$  under a constant volume, yielding  $C_V = 0$ . This implies that there is no heat exchange in the isochore process, which means that this process is adiabatic.  $Q_H$  is

$$Q_H = \int_{T_1}^{T_2} C_P(P, T)dT; \tag{1.11}$$

the output work  $W$  is

$$W = \frac{4}{3\sqrt{\pi}}(S_2^{\frac{3}{2}} - S_1^{\frac{3}{2}})(P_1 - P_4). \tag{1.12}$$

Expanding the entropy and  $C_P$  at large  $T$  and  $P$ ,

$$S = \frac{\pi}{4} T^2 - \frac{1}{4P} - \frac{1}{16\pi T^2} + \dots \tag{1.13}$$

$$C_P = \frac{\pi}{2P^2} T^2 + \frac{1}{8\pi T^2} + \dots \tag{1.14}$$

to obtain the approximate efficiency as

$$\eta = \frac{W}{Q_H} = \left(1 - \frac{P_4}{P_1}\right) \left\{1 - \frac{3}{8P_1} \left(\frac{S_2^{\frac{1}{2}} - S_1^{\frac{1}{2}}}{S_2^{\frac{3}{2}} - S_1^{\frac{3}{2}}}\right) + O\left(\frac{1}{P_1^2}\right)\right\}. \tag{1.15}$$

Actually, we have

$$Q_H = \int_{T_1}^{T_2} C_P(P, T)dT = \int_{T_1}^{T_2} T \frac{\partial S}{\partial T} \Big|_P dT = \int_1^2 T dS. \tag{1.16}$$

Considering the first law of thermodynamics under constant pressure and other parameters except the entropy, we have

$$dM = TdS, \tag{1.17}$$

which yields

$$Q_H = M_2 - M_1, \tag{1.18}$$

$$Q_C = M_3 - M_4, \tag{1.19}$$

so finally we have the exact efficiency

$$\eta = 1 - \frac{M_3 - M_4}{M_2 - M_1}. \tag{1.20}$$

Modern observational results [42–44] have showed that our universe is expanding with acceleration. One method to explain this amazing accelerating expansion is to introduce the so-called dark energy which makes up about 70% of the universe and has negative pressure in order to propel the accelerating expansion of the cosmos. The cosmological constant and scalar field are two kinds of dark energy model. Quintessence is proposed as a spatially homogeneous canonical real scalar field, believed to be a type of candidate of dark energy model with the state parameter  $-1 < \omega_q < 1$ , but the parameter must be restricted to  $-1 < \omega_q < -\frac{1}{3}$  to explain the late-time cosmic acceleration [45–48]. Kiselev [49] obtained an exact solution of the Einstein equation with the quintessence matter surrounding a charged or non-charged black hole. Then, based on Kiselev’s achievement, considerable attention [50–59] has been paid to investigating the thermodynamical properties of black holes surrounded by quintessence, including the influence of quintessence to the critical behavior in the extended phase space of such black holes [60]. Taking into account the dark energy, it would be of interest to investigate whether and how the dark energy would influence the heat engine efficiency of AdS black holes and we believe that this may not only deepen our understanding of black hole thermodynamics but also provide us a new hint to research as regards dark energy.

This paper is organized as follows. In Sect. 2, we give a brief review of RN-AdS black holes surrounded by quintessence, since it is the base of our present work. In Sect. 3, we discuss the influence of quintessence to the heat engine efficiency of charged AdS black holes. In Sect. 4, we will investigate critical black holes as heat engines and the last section is devoted to conclusions and discussions.

## 2 A brief review of thermodynamics of black holes surrounded by quintessence

In this section, we are going to introduce the thermodynamics of RN-AdS black holes surrounded by quintessence by reviewing Ref. [49,60].

The metric of such black holes has the form

$$ds^2 = f(r)dt^2 - f(r)^{-1}dr^2 - r^2(d\theta^2 + \sin^2\theta d\phi^2) \quad (2.1)$$

where  $f(r)$  is

$$f(r) = 1 - \frac{2M}{r} + \frac{Q^2}{r^2} - \frac{a}{r^{3\omega_q+1}} - \frac{\Lambda r^2}{3}; \quad (2.2)$$

the parameter  $\omega_q$  and  $a$  are the state parameter and normalization factor of the quintessence field, respectively.  $r_+$  stands for the event horizon radius meeting the horizon equation  $f(r_+) = 0$ , which yields the black hole mass  $M$

$$M = \frac{r_+}{2} \left( 1 + \frac{Q^2}{r_+^2} - \frac{a}{r_+^{3\omega_q+1}} - \frac{\Lambda r_+^2}{3} \right). \quad (2.3)$$

The Hawking temperature related to the surface gravity  $k$  on the event horizon is

$$T = \frac{k}{2\pi} \quad (2.4)$$

where  $k$  can be calculated by the general formula

$$k = \lim_{r \rightarrow r_+} \left[ -\frac{1}{2} \sqrt{\frac{g^{11}}{-g_{00}}} \frac{\partial g_{00}}{\partial r} \right]. \quad (2.5)$$

Then the Hawking temperature can be computed:

$$T = \frac{f'(r)}{4\pi} = \frac{1}{4\pi} \left( \frac{1}{r_+} - \frac{Q^2}{r_+^3} + \frac{3a\omega_q}{r_+^{2+3\omega_q}} - r_+\Lambda \right). \quad (2.6)$$

By the first law of thermodynamics, we get the Hawking–Bekenstein entropy,

$$S = \int_0^{r_+} \frac{1}{T} \left( \frac{\partial M}{\partial r_+} \right) dr_+ = \pi r_+^2 = \frac{A}{4}; \quad (2.7)$$

$A$  stands for the horizon area. By employing Eq. (1.1), the black hole mass  $M$  can be reexpressed as

$$M = \frac{r_+}{2} \left( 1 + \frac{Q^2}{r_+^2} - \frac{a}{r_+^{3\omega_q+1}} + \frac{8\pi Pr_+^2}{3} \right), \quad (2.8)$$

so the thermodynamic volume  $V$  conjugate to the pressure  $P$  can be derived from Eq. (2.8):

$$V = \left( \frac{\partial M}{\partial P} \right)_{S,Q} = \frac{4\pi r_+^3}{3}. \quad (2.9)$$

To obtain the Smarr relation, when quintessence field is taken into account the first law for the RN-AdS black hole must be modified as follows:

$$dM = TdS + \phi dQ + VdP + \mathcal{A}da, \quad (2.10)$$

the quantity  $\mathcal{A}$  is

$$\mathcal{A} = \left( \frac{\partial M}{\partial a} \right)_{S,Q,P} = -\frac{1}{2r_+^{3\omega_q}}, \quad (2.11)$$

which is conjugate to  $a$ . By a dimensional analysis, the Smarr relation can be derived:

$$M = 2TS + \phi Q - 2VP + (1 + 3\omega_q)\mathcal{A}a \quad (2.12)$$

We have the following equation of state:

$$P = \frac{T}{v} - \frac{1}{2\pi v^2} + \frac{2Q^2}{\pi v^4} - \frac{8^{\omega_q} \times 3a\omega_q}{\pi v^{3(1+\omega_q)}} \quad (2.13)$$

where  $v = 2r_+$  is the specific volume which actually is the double horizon radius of black hole; this differs from the specific volume with dimension  $[L^3]$  defined in traditional thermodynamics. Moreover, we can obtain the critical temperature  $T_c$  and the critical pressure  $P_c$ ,

$$T_c = \frac{1}{\pi v_c} - \frac{8Q^2}{\pi v_c^3} + \frac{8^{\omega_q} \times 9a\omega_q(1 + \omega_q)}{\pi v_c^{3\omega_q+2}}, \quad (2.14)$$

$$P_c = \frac{1}{2\pi v_c^2} - \frac{6Q^2}{\pi v_c^4} + \frac{8^{\omega_q} \times 3a\omega_q(2 + 3\omega_q)}{\pi v_c^{3(1+\omega_q)}}, \quad (2.15)$$

where  $v_c$  is the critical specific volume, which satisfies the equation

$$v_c^2 - 24Q^2 + \frac{9a\omega_q 8^{\omega_q} (3\omega_q + 2)(\omega_q + 1)}{v_c^{3\omega_q - 1}} = 0. \tag{2.16}$$

For  $\omega_q = -\frac{2}{3}$ , we have

$$v_c = 2\sqrt{6}Q, \quad T_c = \frac{\sqrt{6}}{18\pi Q} - \frac{a}{2\pi}, \quad P_c = \frac{1}{96\pi Q^2}, \tag{2.17}$$

and when  $\omega_q = -1$ , we obtain

$$v_c = 2\sqrt{6}Q, \quad T_c = \frac{\sqrt{6}}{18\pi Q}, \quad P_c = \frac{1}{96\pi Q^2} + \frac{3a}{8\pi}. \tag{2.18}$$

For other values of state parameter  $\omega_q$ , Eq. (2.16) cannot be analytically solved so that we cannot get the analytical formula for  $v_c$ ,  $T_c$  and  $P_c$ , and numerical methods must be adopted for help. On the other hand, we have the ratios

$$\begin{aligned} \left. \frac{P_c v_c}{T_c} \right|_{\omega_q = -\frac{2}{3}} &= \frac{3}{8 - 12\sqrt{6}aQ}, & \left. \frac{P_c v_c}{T_c} \right|_{\omega_q = -1} \\ &= \frac{3}{8} (1 + 36aQ^2), \end{aligned} \tag{2.19}$$

which do not keep constant as the charged AdS-RN black hole in the spacetime without quintessence does but are dependent on the factor  $a$  and charge  $Q$ , and this result reflects the effects of the quintessence field on the black hole thermodynamics. One should note that when  $a = 0$ , the ratio in Eq. (2.19) will be reduced to

$$\frac{P_c v_c}{T_c} = \frac{3}{8}, \tag{2.20}$$

which keeps the same value as the van der Waals liquid–gas system. From another perspective, we can introduce a new temperature, denoted as  $w$ , for  $\omega_q = -\frac{2}{3}$ :

$$w = T_c + \frac{a}{2\pi}, \tag{2.21}$$

which is called the shifted temperature and the universal ratio value can be obtained:

$$\frac{P_c v_c}{w} = \frac{3}{8}. \tag{2.22}$$

For  $\omega_q = -1$ , a similar procedure can be employed to obtain the universal ratio value.

### 3 The efficiency of heat engines influenced by quintessence

In this section, we will probe the effects of dark energy (i.e. quintessence field in this paper) on the efficiency of RN-AdS black holes as the heat engine defined in Fig. 3. From Eqs. (2.7), (2.6) and (1.1), the Hawking temperature can be rewritten as

$$T = \frac{S^{-\frac{3}{2}(1+\omega_q)} \left( S^{\frac{3\omega_q}{2}} (-\pi Q^2 + S + 8PS^2) + 3a\pi^{\frac{1+3\omega_q}{2}} \sqrt{S}\omega_q \right)}{4\sqrt{\pi}}, \tag{3.1}$$

and then the heat capacity can be calculated by employing Eq. (3.1):

$$\begin{aligned} C &= T \frac{\partial S}{\partial T} \\ &= \frac{-2 \left( -\sqrt{\pi} + 2 \frac{\partial P}{\partial T} \sqrt{S} \right) S \left( S^{3\omega_q/2} (-\pi Q^2 + S + 8PS^2) + 3a\pi^{\frac{1+3\omega_q}{2}} \sqrt{S}\omega_q \right)}{\sqrt{\pi} S^{\frac{3\omega_q}{2}} (3\pi Q^2 + S(8PS - 1)) - 3a\pi^{\frac{3\omega_q+2}{2}} \sqrt{S}\omega_q (3\omega_q + 2)}. \end{aligned} \tag{3.2}$$

The heat capacity  $C_P$  under constant pressure  $P$  can be obtained by the condition

$$\frac{\partial P}{\partial T} = 0. \tag{3.3}$$

We substitute Eq. (3.3) into Eq. (3.2) to get  $C_P$ ,

$$C_P = \frac{2S^{\frac{3\omega_q+2}{2}} (S + 8PS^2 - \pi Q^2) + 6a\pi^{\frac{3\omega_q+2}{2}} \sqrt{\frac{3}{2}}\omega_q}{S^{\frac{3\omega_q}{2}} (3\pi Q^2 + S(8PS - 1)) - 3a\pi^{\frac{3\omega_q+2}{2}} \sqrt{S}\omega_q (3\omega_q + 2)}. \tag{3.4}$$

To get the heat capacity  $C_V$  under constant volume, we can substitute  $\left. \frac{\partial P}{\partial T} \right|_V$  into Eq. (3.2) and we have

$$\left. \frac{\partial P}{\partial T} \right|_V = \frac{\sqrt{\pi}}{2\sqrt{S}} \Rightarrow C_V = 0. \tag{3.5}$$

The equation of state (2.13) and the entropy formula (2.7) are used in the calculations above. Both the RN-AdS black holes and the RN-AdS black holes surrounded by quintessence have heat capacity  $C_V = 0$ , which means that the quintessence would not affect the black hole heat capacity under the fixed thermodynamic volume, while  $C_P$  will be affected by the quintessence field. Zero  $C_V$  suggests that there is no heat exchange in the isochoric process ( $2 \rightarrow 3$  and  $4 \rightarrow 1$  in Fig. 3), so that we only need to calculate the heat  $Q_H$  along the process  $1 \rightarrow 2$ , which can be computed as

$$\begin{aligned}
 Q_H &= \int_{T_1}^{T_2} C_P(P_1, T) dT = \int_{r_1}^{r_2} C_P(P_1, T) \frac{\partial T}{\partial r} dr \\
 &= \frac{1}{6} \left( \frac{3\pi Q^2 + S_2(3 + 8P_1S_2)}{\sqrt{\pi S_2}} - 3a\pi^{\frac{3\omega_q}{2}} S_2^{-\frac{3\omega_q}{2}} \right) \\
 &\quad - \frac{1}{6} \left( \frac{3\pi Q^2 + S_1(3 + 8P_1S_1)}{\sqrt{\pi S_1}} - 3a\pi^{\frac{3\omega_q}{2}} S_1^{-\frac{3\omega_q}{2}} \right). \tag{3.6}
 \end{aligned}$$

The output work  $W$ , i.e. the area of the rectangle, is

$$W = \frac{4}{3\sqrt{\pi}} (S_2^{\frac{3}{2}} - S_1^{\frac{3}{2}}) (P_1 - P_4) \tag{3.7}$$

and now the efficiency can be derived as

$$\begin{aligned}
 \eta &= \frac{W}{Q_H} = \left( 1 - \frac{P_4}{P_1} \right) \\
 &\quad \times \frac{1}{1 + \frac{3(\sqrt{S_1 S_2} - \pi Q^2)}{8\sqrt{S_1 S_2} (S_1 + S_2 + \sqrt{S_1 S_2}) P_1} + \frac{3a\pi^{\frac{1+3\omega_q}{2}} (S_2^{-\frac{3\omega_q}{2}} - S_1^{-\frac{3\omega_q}{2}})}{8(S_1^{\frac{3}{2}} - S_2^{\frac{3}{2}}) P_1}}}. \tag{3.8}
 \end{aligned}$$

One can directly check that this formula indeed equals the efficiency formula expressed by the black hole mass  $M$  in Eq. (1.20). Focusing on the large volume branch of solutions and therefore neglecting the charge  $Q$  to leading order, we can obtain

$$\begin{aligned}
 \eta &= \left( 1 - \frac{P_4}{P_1} \right) \left\{ 1 + \frac{1}{P_1} \left( \frac{3a\pi^{\frac{1+3\omega_q}{2}} (S_1^{-\frac{3\omega_q}{2}} - S_2^{-\frac{3\omega_q}{2}})}{8(S_1^{\frac{3}{2}} - S_2^{\frac{3}{2}}) P_1} \right) \right. \\
 &\quad \left. - \frac{3}{8P_1} \left( \frac{S_2^{\frac{1}{2}} - S_1^{\frac{1}{2}}}{S_2^{\frac{3}{2}} - S_1^{\frac{3}{2}}} \right) + \mathcal{O} \left( \frac{1}{P_1^2} \right) \right\}. \tag{3.9}
 \end{aligned}$$

We consider the condition  $a = 0$ , which means that the quintessence field disappears such that the metric (2.1) can be reduced to pure RN-AdS black holes, and then the efficiency (3.9) would be simplified to

$$\eta = \left( 1 - \frac{P_4}{P_1} \right) \left\{ 1 - \frac{3}{8P_1} \left( \frac{S_2^{\frac{1}{2}} - S_1^{\frac{1}{2}}}{S_2^{\frac{3}{2}} - S_1^{\frac{3}{2}}} \right) + \mathcal{O} \left( \frac{1}{P_1^2} \right) \right\}, \tag{3.10}$$

which coincides with the result shown in Ref. [26]. The normalization factor  $a$  is related to the density  $\rho_q$  of the quintessence field by

$$\rho_q = -\frac{a}{2} r^{3(\omega_q+1)}. \tag{3.11}$$

Equation (3.11) implies that for a negative state parameter  $\omega_q$ , the factor  $a$  must be limited to positive values to keep the density positive. For the entropy, we have  $S_2 > S_1$  and the negative  $\omega_q$  will keep  $S_2^{-3\omega_q/2} > S_1^{-3\omega_q/2}$ , which makes the second term in the brace of Eq. (3.9) positive, so that the efficiency of the heat engine of the RN-AdS black holes surrounded by quintessence is higher than the efficiency (Eq. 3.10) of the pure RN-AdS black holes as a heat engine. In other words, the quintessence field, as a kind of dark energy model, can promote the heat engine efficiency of the charged AdS black holes provided that  $\omega_q < 0$ . Considering that the term including a negative  $\omega_q$  (parameter  $a$  is positive) in the black hole mass formula (2.8) has a negative contribution to  $\partial M/\partial V$ , we find that our result is consistent with the result concluded in Ref. [39], which presents some general considerations for holographic heat engines for both static and rotating black holes, and which states that for the black holes with  $C_V = 0$ , any quantity contributing negatively to  $\partial M/\partial V$  will lead to a larger efficiency. Furthermore, the efficiency of the Carnot engine is

$$\eta_c = 1 - \frac{T_C}{T_H} = 1 - \frac{T_4(P_4, S_1)}{T_2(P_1, S_2)}. \tag{3.12}$$

Now that all the quantities we need for the discussion have been obtained above, it is necessary and important to investigate how the efficiency changes under the different normalization factor  $a$ , state parameter  $\omega_q$ , black hole entropy  $S_2$  related to volume and the higher pressure  $P_1$ .

We plot the efficiency  $\eta$  and the ratio between  $\eta$  and Carnot efficiency  $\eta_c$  by employing Eqs. (3.8) and (3.12) in Fig. 4, which shows us that the heat engine efficiency  $\eta$  (right figure of Fig. 4) monotonously decreases with the entropy  $S_2$  (or volume  $V_2$ ) increasing, implying that the bigger volume difference between the smaller black holes ( $V_1$ ) and the bigger black holes ( $V_2$ ) correspond to a lower efficiency. On the other hand, the decrease of the efficiency gradually becomes slower as the volume difference becomes bigger till the efficiency becomes constant. Moreover, we see that when all the other parameters are fixed, the heat engine with a bigger normalization factor  $a$  always has the higher efficiency  $\eta$ ; this fact tells us that the quintessence field with the bigger density  $\rho_q$  would more significantly improve (or influence) the black hole heat engine efficiency. As we can see in the following parts of this present paper, the factor  $a$  should be bounded in order to have a heat engine with the efficiency  $\eta < 1$ . The left figure related to the  $\frac{\eta}{\eta_c}$  of Fig. 4 behaves similar to the right one but their implications are distinct. We can see that  $\frac{\eta}{\eta_c} < 1$  always holds for three different  $a$  at any entropy  $S_2$ , and this result is consistent with the fact in the traditional thermodynamics that the Carnot heat engine has the highest efficiency—otherwise the second law of the thermodynamics will be broken. On the other hand, the ratio

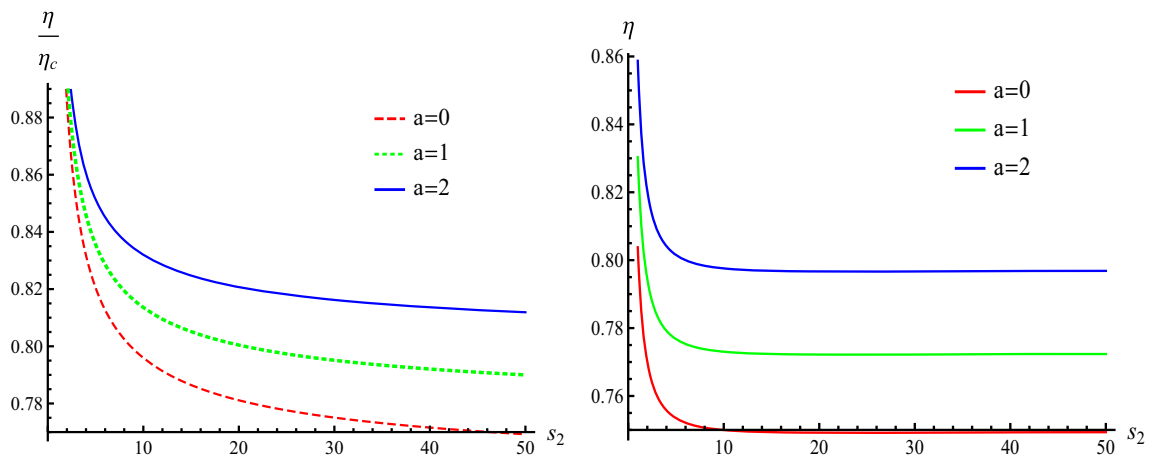


**Fig. 4** The two figures above are plotted at three different fixed normalization factors  $a$ ; here we take  $P_1 = 4, P_4 = 1, S_1 = 1, Q = 1$  and state parameter  $\omega_q = -1$ . The *left* figure corresponds to the ratio between efficiency  $\eta$  and  $\eta_c$ , the *right* one to the efficiency  $\eta$

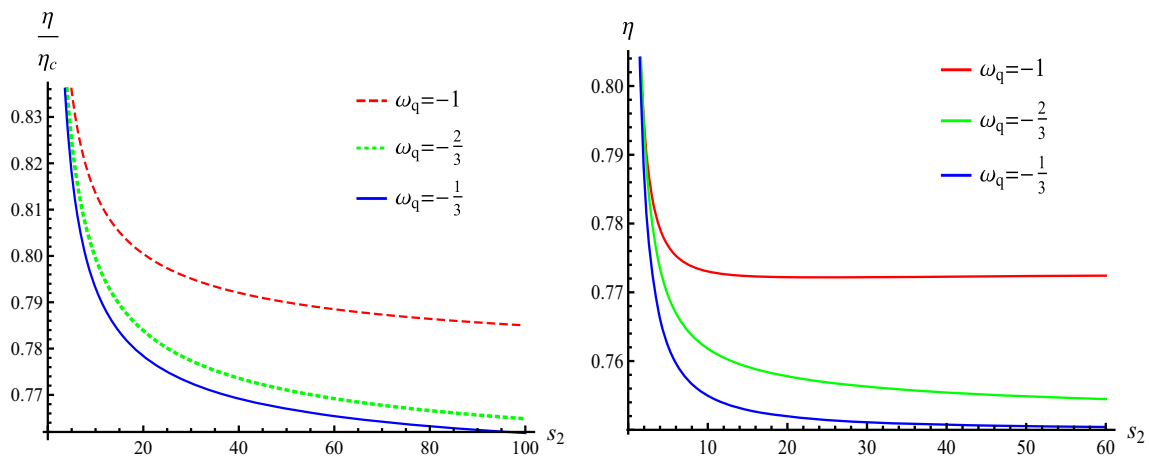


**Fig. 5** The two figures above are plotted at three different fixed state parameters  $\omega_q$ , here we take  $P_1 = 4, P_4 = 1, S_1 = 1, Q = 1$  and normalization factor  $a = 1$ . The *left* figure corresponds to the ratio between the efficiencies  $\eta$  and  $\eta_c$ , the *right* one to efficiency  $\eta$

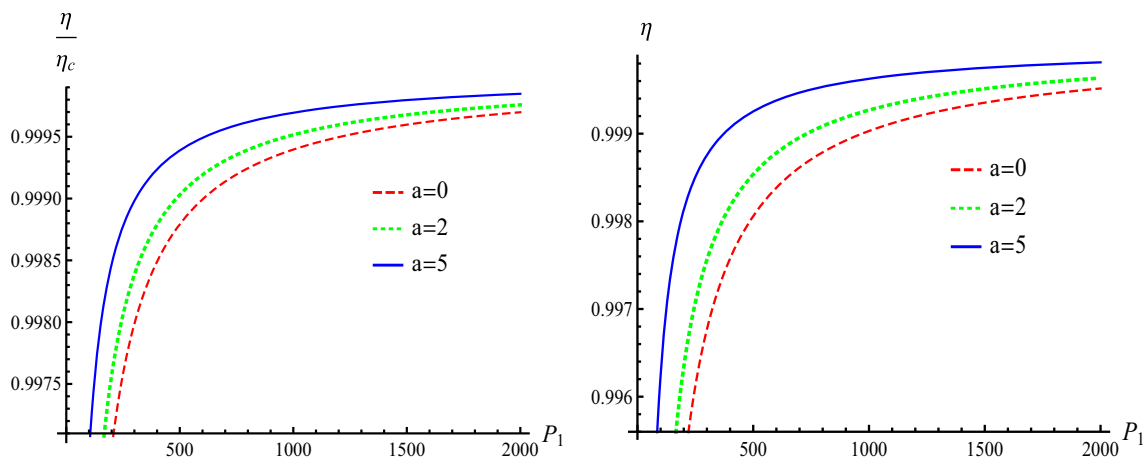
$\eta/\eta_c$  monotonously decreases with the increase of entropy  $S_2$ , which suggests that the bigger the black hole is, the difference between the bigger actual efficiency  $\eta$  and the idealized highest efficiency  $\eta_c$ ; in other words, the energy utilization rate is smaller.

Figure 5 is plotted under three different state parameters  $\omega_q$ . The curves in this figure are highly similar to that in Fig. 4; therefore similar discussions for Fig. 4 can be used in this situation but there is one feature we should point out. Figure 5 shows that, for a bigger state parameter  $\omega_q$ , the corresponding heat engine efficiency is smaller. This result is apparent since the quintessence field density  $\rho_q$  decreases with the parameter  $\omega_q$  increasing from  $-1$  to  $0$  at the constant factor  $a$  as shown by Eq. (3.11).

On the other hand, we would like to investigate how the  $\eta$  and  $\eta_c$  change under the change of pressure  $P_1$  by plotting Fig. 6. We can see from the right figure that the efficiency monotonously increases as the  $P_1$  increases but the efficiency

would not approach the value 1 within the limited  $P_1$ . The left figure shows that the efficiency would get closer and closer to the maximum efficiency value of the Carnot heat engine with the increase of  $P_1$ . Apparently, both  $\eta$  and  $\eta_c$  would approach 1 when  $P_1$  goes to infinity.

Now it is time to probe how the quintessence field influences the efficiency. We plot figures of  $\eta$  and  $\eta/\eta_c$  in Fig. 7 under the change of the normalization factor  $a$  at three fixed different state parameters. The figures show that the efficiency  $\eta$  monotonously increase with the increase of  $a$  for all three  $\omega_q$ , while, for  $\eta/\eta_c$ , only the curve corresponding to  $\omega_q = -\frac{1}{3}$  monotonously increases and the other two begin with a decrease and then increase. One should note that both  $\eta$  and  $\eta/\eta_c$  would exceed the maximum value 1 and this phenomenon is forbidden to appear by the laws of thermodynamics. In order to preserve the thermodynamics laws, the factor  $a$ , or quintessence field density  $\rho_q$  must be constrained in a range which can be roughly observed from



**Fig. 6** The two figures above are plotted at three different fixed normalization factors  $a$ , here we take  $P_2 = 4, S_1 = 1, S_2 = 4, Q = 1$  and state parameter  $\omega_q = -1$

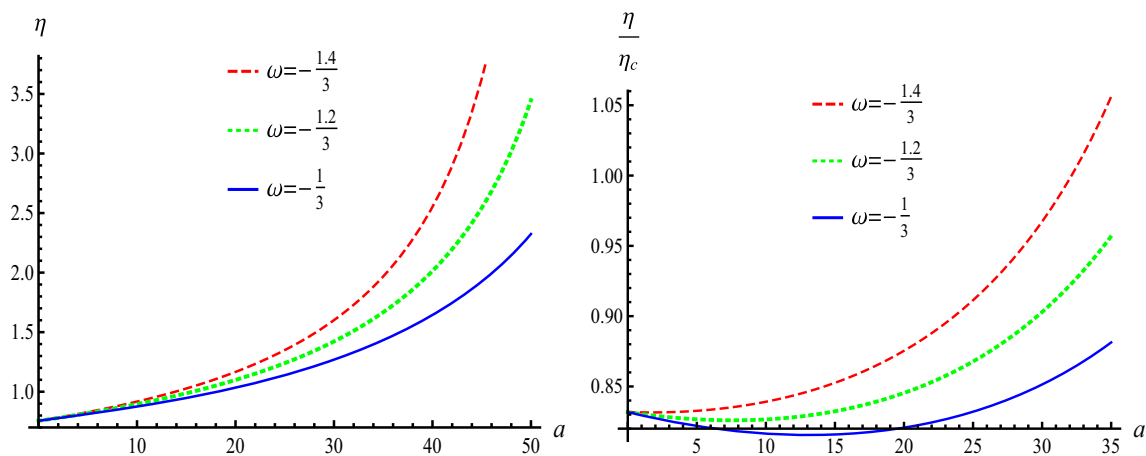


**Fig. 7** The two figures above are plotted at three different fixed state parameter  $\omega_q$ , here we take  $P_1 = 4, P_4 = 1, S_1 = 1, S_2 = 4, Q = 1$

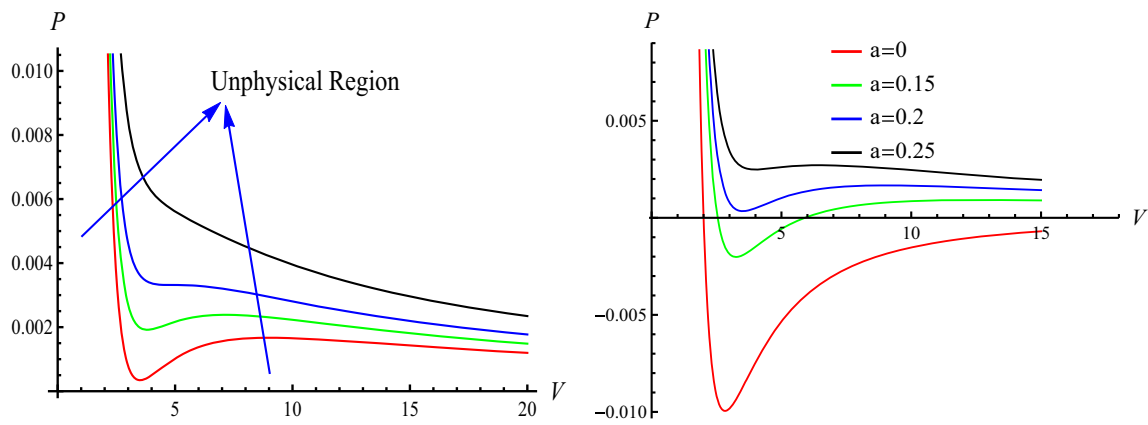
Fig. 7. In fact, Eq. (2.6) shows that a big enough factor  $a$  or electric charge  $Q$  can lead to a negative temperature, which is unphysical. On the other hand, since the thermodynamical cycle in Fig. 7 is fixed in the  $P$ - $V$  plane, the increase of the parameter  $a$  will make the unphysical region in the  $P$ - $V$  plane move to the right so that the cycle will be shifted from the physical region to an unphysical region and this plays a role in the occurrence of  $\eta > 1$  and  $\eta/\eta_c > 1$  as we show in Fig. 7. Figures 8 and 9 are plotted to demonstrate the shift of the thermodynamical cycle fixed in the  $P$ - $V$  plane from a physical region to an unphysical region, which serves as a possible reason discussed here for the unphysical value of  $\eta$  and  $\eta/\eta_c$ .

Figure 10 presents the efficiencies  $\eta$  and  $\eta/\eta_c$  under the change of state parameter  $\omega_q$ . As we discussed in the previous part of this paper, the higher field density  $\rho_q$  corresponds to the higher efficiency as shown in the left figure of Fig. 10. While for the value of  $\eta/\eta_c$ , which is bigger when the related factor  $a$  is bigger at the range  $-1 \leq \omega_q \leq -0.462945$  as

portrayed by the right figure of Fig. 10. But what is interesting is that at the range of  $-0.462945 \leq \omega_q \leq 0$ , we have the contrary result that the bigger  $a$  will lead to a smaller value of  $\eta/\eta_c$ .

At this point, we have arrived at the conclusion that the quintessence field (as the famous scalar field model of dark energy) with negative state parameter  $\omega_q$  can promote the efficiency of the heat engine defined in the extended phase space of the charged AdS black holes, but this result should be checked, since different schemes can be chosen; whether the quintessence field can improve the efficiency of the heat engine operating in a new scheme is unknown yet. One choice of the new scheme is to specify the temperatures  $T_1$  and  $T_2$  and pressures  $P_1$  and  $P_4$ , which can be used to calculate the black hole mass—hence Eq. (1.20) is convenient to use to compute the efficiency. For simplicity, we only discuss the quintessence field with  $\omega_q = -1$  and  $\omega_q = -2/3$  due to our ability to analytically solve the equation of state (Eq. 2.13) to get the value of the mass. Figure 11 is plotted to illustrate the





**Fig. 8** For the left plot, the left region and the bottom area of the red isotherm, which represents  $T = 0$ , corresponds to negative temperature isotherms which are unphysical. In the right plot, we plot four isotherms with temperature  $T = 0$ , and we see that the isotherms will move to the right with the increase of the parameter  $a$ , i.e. the unphysical region

will be shifted from left to the right when  $a$  grows such that the cycle fixed in the plane will always be shifted to the unphysical region if  $a$  is big enough, and this may serve as the origin for  $\eta > 1$  and  $\eta/\eta_c > 1$  as shown in Fig. 7. Here we take  $\omega_q = -\frac{2}{3}$

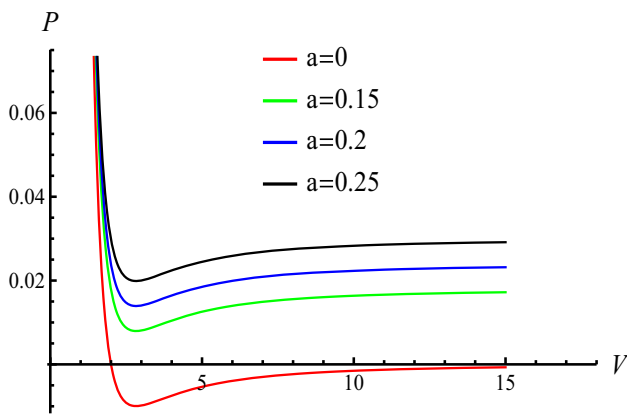


**Fig. 9** The four  $T = 0$  isotherms are plotted in the case  $\omega_q = -1$ . With the increase of the parameter  $a$ , the isotherms with fixed temperature ( $T = 0$  here) will move to the upper region of the  $P$ - $V$  plane such that the fixed thermodynamical cycle would be shifted from the physical region to the unphysical region as the cycle with  $\omega_q = -2/3$  does

behavior of the efficiencies  $\eta$  and  $\eta_c$ , which will increase with growing normalization factor  $a$  (or dark energy density), and this result is consistent with the conclusion we have obtained in the previous part of the present paper. From the plots we see that the factor  $a$  should be restricted to keep the efficiency physical, i.e.  $\eta < \eta_c$ .

#### 4 Critical black holes as heat engines

The latest progress of the black hole heat engine research made by Johnson [61] demonstrates that the black hole heat engine defined in the  $P$ - $V$  plane with the thermodynamical quantities at the critical point to approach the Carnot limit with the increase of the electric charge  $Q$  at finite power is possible. This discovery is amazing, since the Carnot heat engine, setting an upper bound on the efficiency of a heat engine is an ideal, reversible engine of which a single cycle

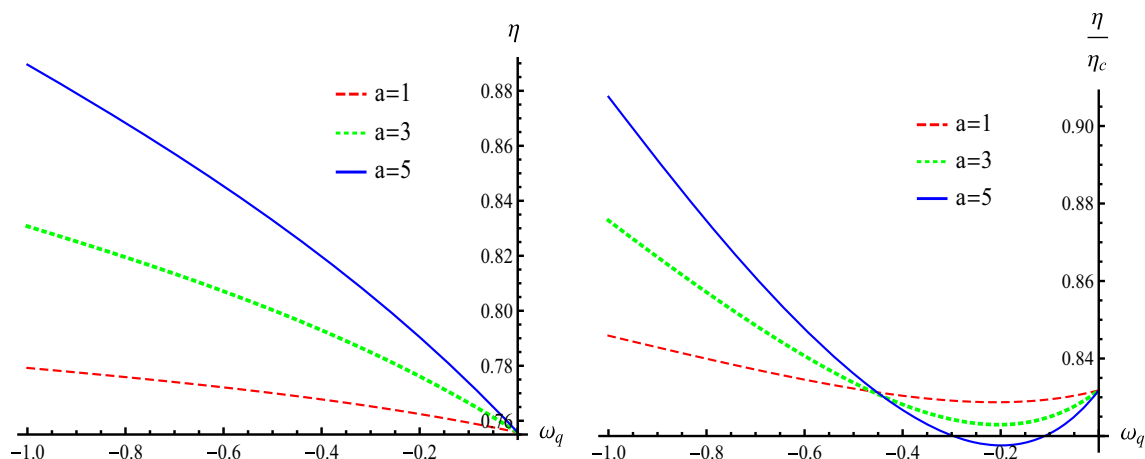


**Fig. 10** The two figures above are plotted at three different fixed normalization factors  $a$ , here we take  $P_1 = 4, P_4 = 1, S_1 = 1, S_2 = 4, Q = 1$

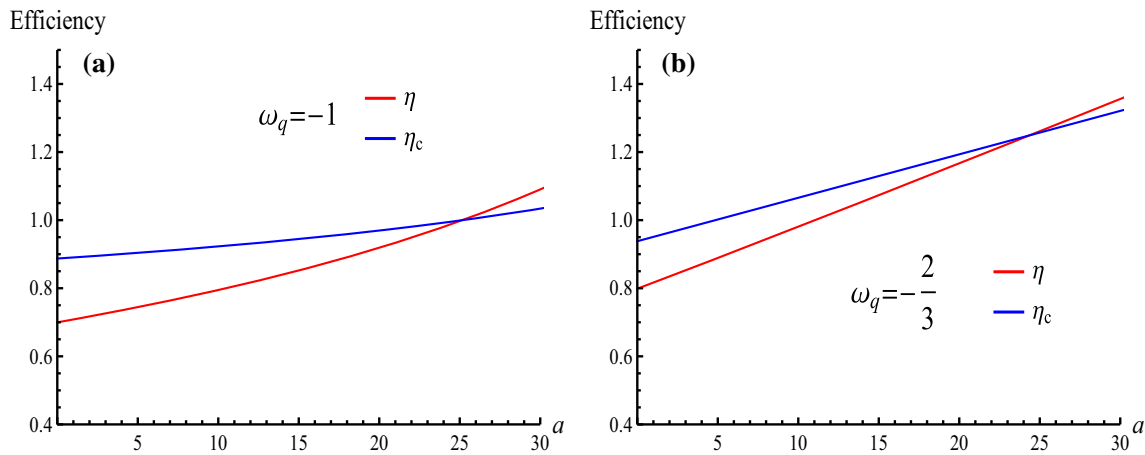


**Fig. 11** **a** The left plot is plotted by specifying  $T_1 = 30, T_2 = 80, P_1 = P_2 = 10, P_3 = P_4 = 3$ , charge  $Q = 1$  and state parameter  $\omega_q = -1$ . **b** The right plot is plotted by specifying  $T_1 = 3, T_2 = 10, P_1 = P_2 = 0.5, P_3 = P_4 = 0.1$ , charge  $Q = 1$  and state parameter  $\omega_q = -\frac{2}{3}$

must be performed in infinite time which is impractical and so the Carnot engine has zero power. Inspired by this work, we find that the RN-AdS black hole surrounded by quintessence with the state parameter  $\omega_q = -1$  can be treated in a similar way, in which one can solve the problem shown in Fig. 7, i.e. the  $\eta > 1$  and  $\eta/\eta_c > 1$ . The core of this way is to find a thermodynamic cycle which keeps the temperature non-negative at any given  $a$  or electric charge  $Q$ . To achieve this goal, the position of the cycle should be changed with the change of the parameter  $a$  or charge  $Q$  rather than be fixed in the  $P$ - $V$  plane, and thereby the scaling behavior of the thermodynamical quantities must be used to define the thermodynamical cycle. We here would use the critical pressure  $P_c$ , the critical temperature  $T_c$  and the critical specific volume  $v_c$  with the state parameter  $\omega_q = -1$  in Eq. (2.18). There are several ways for making such a choice, which is essential and crucial to the property of the heat engines as we can see in the following discussions, and just two families are chosen here for illustration. Figure 12 is the heat engine constructed near the critical point we are going to investigate in this section.

#### 4.1 Heat engine model 1

In this section, we construct the heat engines with the following choice:

$$V_2 = V_3 = V_c = \frac{4\pi}{3} \left(\frac{v_c}{2}\right)^3, \quad P_3 = P_4 = P_c, \quad P_1 = P_2 = \frac{3}{2}P_c \quad (4.1)$$

$$V_1 = V_4 = \alpha V_c, \quad S_2 = S_3 = \pi \left(\frac{3V_c}{4\pi}\right)^{\frac{2}{3}}, \quad S_1 = S_4 = \pi \left(\frac{3\alpha V_c}{4\pi}\right)^{\frac{2}{3}}, \quad (4.2)$$

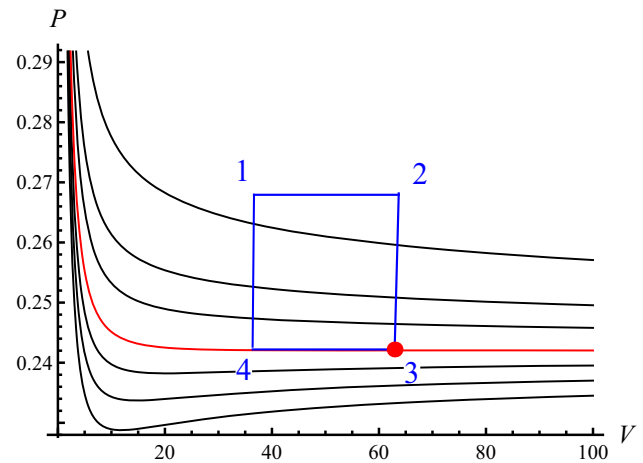


**Fig. 12** The corner 3 of the engine cycle is placed at the critical point (i.e.  $T_c = 0.0433, P_c = 0.242$  and  $V_c = 61.56$ ), and the red curve stands for the  $T = T_c$  isotherm, here we take  $a = 2, Q = 1$

where the dimensionless factor  $\alpha$  is a constant restricted to  $0 < \alpha < 1$  to keep  $V_1 = V_4$  smaller than  $V_c$ . By employing Eqs. (4.1), (4.2), (2.18) and (3.9), the efficiency  $\eta$  can be reduced to

$$\eta = \frac{(1 + 36aQ^2)(\alpha^{1/3} + \alpha^{2/3} + \alpha)}{3(12aQ^2 + 5)\alpha^{1/3} + 3(1 + 12aQ^2)(\alpha + \alpha^{2/3}) - 2}, \quad (4.3)$$

and the Carnot efficiency is

$$\eta_c = 1 - \frac{T_4(S_4, P_4)}{T_2(S_2, P_2)} = \frac{2 - 12\alpha^{2/3} + 19\alpha + 108aQ^2\alpha - 6\alpha^{4/3}}{19\alpha + 108aQ^2\alpha}. \quad (4.4)$$

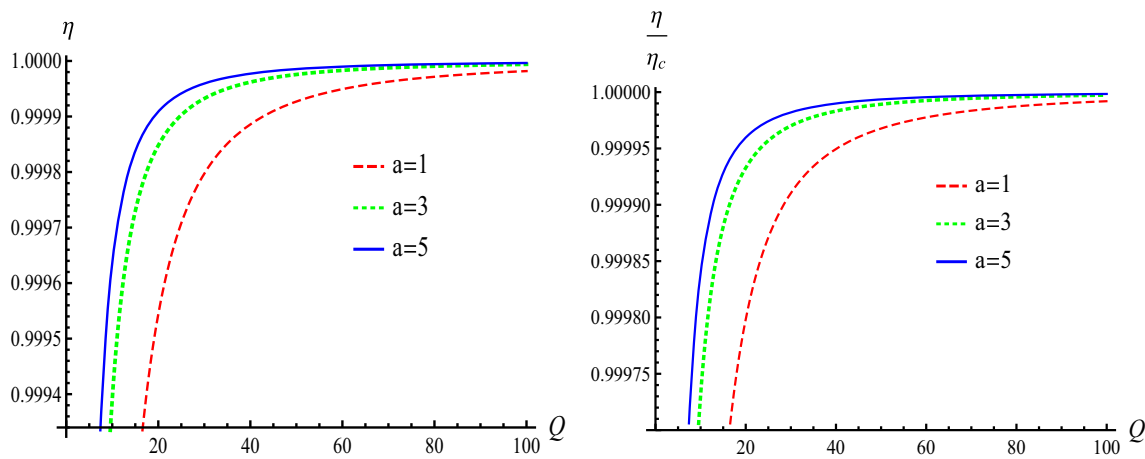


**Fig. 13** The two figures above are plotted under the change of the electric charge  $Q$  at three different fixed normalization factors  $a$ , here we take  $\alpha = \frac{1}{8}$

To gain a better understanding of how the charge  $Q$  influences the efficiency, we carry out a large  $Q$  expansion for both  $\eta$  and  $\eta_c$ .

$$\eta = 1 - \frac{23}{126aQ^2} + \frac{1219}{31,752a^2Q^4} - \frac{64,607}{8,001,504a^3Q^6} + \mathcal{O}(Q^{-7}), \tag{4.5}$$

$$\eta_c = 1 - \frac{11}{108aQ^2} + \frac{209}{11,664a^2Q^4} - \frac{3971}{1,259,712a^3Q^6} + \mathcal{O}(Q^{-7}), \tag{4.6}$$

where we have taken  $\alpha = \frac{1}{8}$  for simplicity. The large  $Q$  expansions for  $\eta$  and  $\eta_c$  indicate that both  $\eta$  and  $\eta_c$  will approach value 1 when  $Q$  goes to infinity, and no unphysical efficiency values appear. We plot  $\eta$  and  $\eta/\eta_c$  in Fig. 13 under the change of the electric charge  $Q$ . The figures show that the efficiencies  $\eta$  and  $\eta/\eta_c$  increase with growing electric charge, and  $\eta$  will approach the Carnot efficiency  $\eta_c$ , which is the maximum value of the efficiency, and which suggests that approaching the Carnot limit is possible as Johnson found in Ref. [61]. In practice, on account of the fact that the electric charge  $Q$  should be finite, the efficiency  $\eta < 1$ , which is allowed by thermodynamics laws, and increasing  $Q$  is supposed to be a way to promote the heat engine efficiency. Furthermore, we would like to expand  $\eta$  and  $\eta_c$  at large parameter  $a$  with  $\alpha = \frac{1}{8}$ :

$$\eta = 1 - \frac{23}{126aQ^2} + \frac{1219}{31,752a^2Q^4} - \frac{64,607}{8,001,504a^3Q^6} + \mathcal{O}(a^{-4}), \tag{4.7}$$

$$\eta_c = 1 - \frac{11}{108aQ^2} + \frac{209}{11,664a^2Q^4}$$

$$- \frac{3971}{1,259,712a^3Q^6} + \mathcal{O}(a^{-4}). \tag{4.8}$$

Interestingly, the expansion formulas at large  $a$  are exactly the same as the formulas of the large  $Q$  expansion, and this coincidence arises from the fact that parameter  $a$  and charge  $Q$  are always bonded together in the form of  $aQ^2$ . We draw the diagram of  $\eta$  and  $\eta/\eta_c$  under the change of factor  $a$ , as we plot in Fig. 14 and no unphysical efficiency values appear. So far, the problem of  $\eta > 1$  and  $\eta/\eta_c > 1$  demonstrated by Fig. 7 for large parameter  $a$  has been solved by making some special choices of the thermodynamical quantities listed in Eqs. (4.1) and (4.2) near the critical point.

To demonstrate how the approach to the Carnot efficiency is affected by the presence of the quintessence field, it would be useful here to discuss the heat engines when the normalization factor  $a = 0$  (i.e. the quintessence field is absent) under the choice of the thermodynamical quantities listed in Eqs. (4.1) and (4.2), which generate a heat engine with an efficiency which is independent of charge  $Q$ . From Eqs. (4.3) and (4.4), it is immediate to get  $\eta$  and  $\eta_c$  under the condition of  $a = 0$ ,

$$\eta = \frac{\alpha^{1/3} + \alpha^{2/3} + \alpha}{3(5\alpha^{1/3} + \alpha^{2/3} + \alpha) - 2}, \tag{4.9}$$

$$\eta_c = \frac{2 - 12\alpha^{2/3} + 19\alpha - 6\alpha^{4/3}}{19\alpha}. \tag{4.10}$$

Obviously, both  $\eta$  and  $\eta_c$  are constant and only depend on the dimensionless constant factor  $\alpha = \frac{V_1}{V_2}$ . One should be aware that the factor  $\alpha$  must be chosen appropriately to avoid the occurrence of unphysical values of the efficiency. Once  $\alpha$  is selected, the efficiency is a constant, which cannot be influenced by the charge  $Q$  if the quintessence field is absent (i.e.  $a = 0$ ); otherwise, the efficiency will be dependent on the normalization factor  $a$  and charge  $Q$ , which provides a possible way to approach the Carnot limit at finite power.

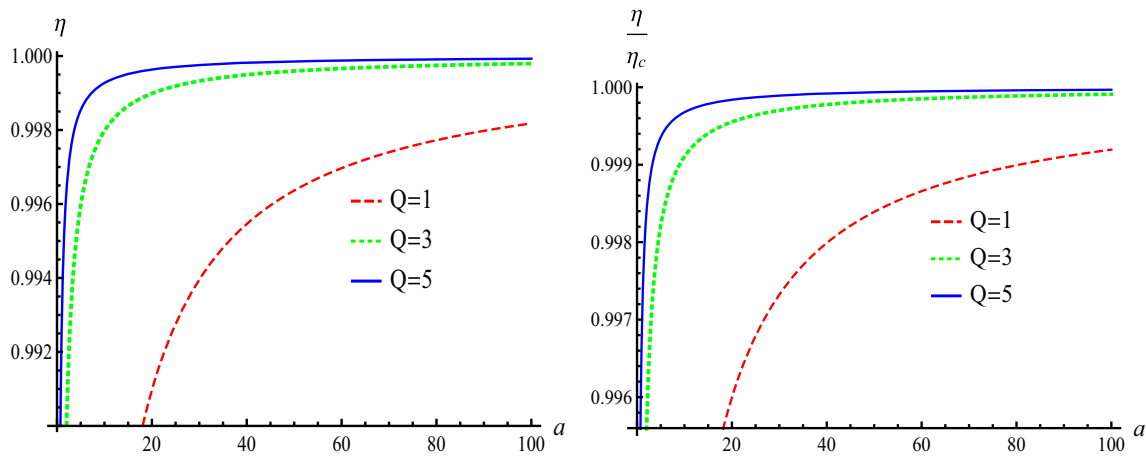


**Fig. 14** The two figures above are plotted under the change of the normalization factor  $a$  at three different fixed electric charges  $Q$ , here we take  $\alpha = \frac{1}{8}$

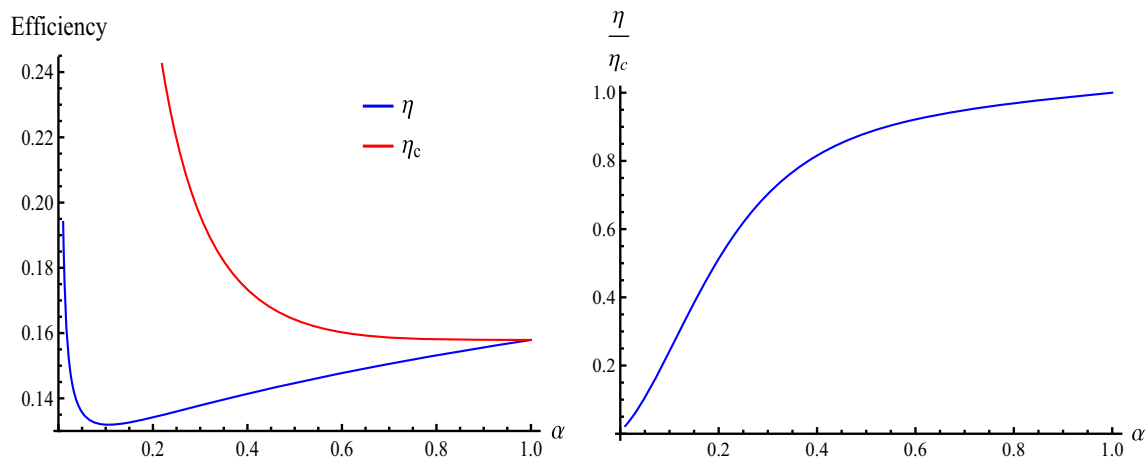


**Fig. 15** The behavior of the efficiency  $\eta$ , the Carnot efficiency  $\eta_c$  and the ratio  $\frac{\eta}{\eta_c}$  under the condition of  $a = 0$

Figure 15 demonstrates the behavior of the efficiency and the ratio  $\eta/\eta_c$  under the change of  $\alpha$ . There is a problem that should be pointed out in the left plot of Fig. 15: when  $\alpha = 1$ , the efficiency  $\eta$  and the Carnot efficiency  $\eta_c$  obey the relation

$$\eta = \eta_c = \frac{3}{19}. \tag{4.11}$$

However,  $\alpha = 1$  means that  $V_1 = V_2$ , which will lead to zero work  $W$ , which can be calculated as

$$W = (P_1 - P_4)(V_2 - V_1) = \frac{Q(1 - \alpha)}{4\sqrt{6}} = 0 \quad (\alpha = 1). \tag{4.12}$$

At the same time, we have

$$Q_H = -\frac{Q(2 + \alpha^{1/3}(12\alpha^{1/3} + 3\alpha - 17))}{4\sqrt{6}\alpha^{1/3}} = 0 \quad (\alpha = 1), \tag{4.13}$$

and the limit of  $\alpha \rightarrow 1$  will give us the nonzero and finite efficiency

$$\eta = \eta_c = \lim_{\alpha \rightarrow 1} \frac{W}{Q_H} = \frac{3}{19} \tag{4.14}$$

although the area of engine cycle has shrunk to zero. The problem arises from the work  $W$  done by the heat engine not being fixed as a constant and the next section is devoted to an investigation of a new heat engine with a thermodynamical cycle which has constant area such that the problem occurring above could be avoided.

#### 4.2 Heat engine model 2

The heat engine discussed in this section is constructed by the following choices of the thermodynamical quantities:

$$V_2 = V_3 = V_c = \frac{4\pi}{3} \left(\frac{v_c}{2}\right)^3, \quad P_3 = P_4 = P_c.$$

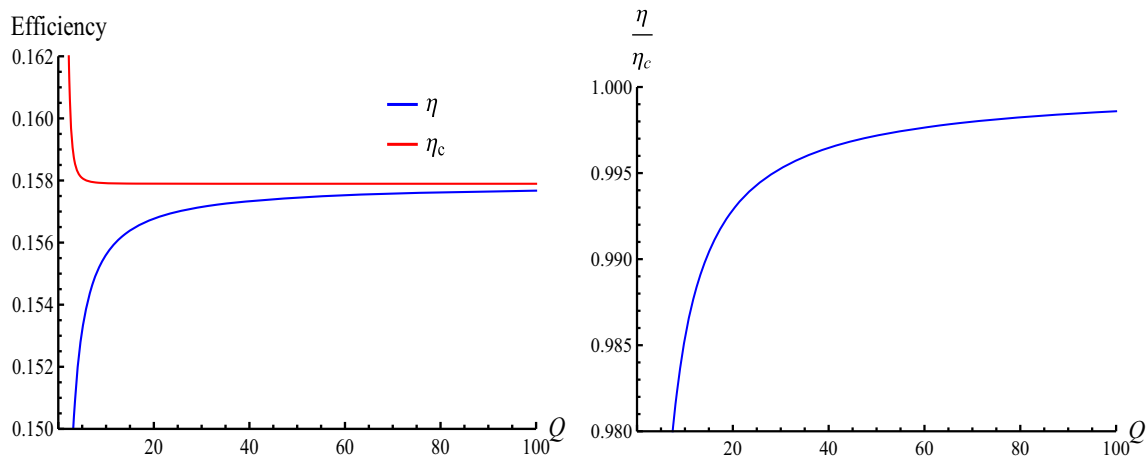


**Fig. 16** The behavior of the efficiency  $\eta$ , the Carnot efficiency  $\eta_c$  and the ratio  $\frac{\eta}{\eta_c}$  as the function of  $Q$

$$P_1 = P_2 = \frac{3(1 + 24aQ^2)}{2(1 + 36aQ^2)} P_c, \tag{4.15}$$

$$V_1 = V_4 = V_c \left(1 - \frac{L}{Q}\right), \quad S_2 = S_3 = \pi \left(\frac{3V_c}{4\pi}\right)^{\frac{2}{3}},$$

$$S_1 = S_4 = \pi \left(\frac{3V_1}{4\pi}\right)^{\frac{2}{3}}, \tag{4.16}$$

where  $L$  is a constant, restricted to  $0 < \frac{L}{Q} < 1$ , and the work is

$$W = (P_1 - P_4)(V_2 - V_1) = \frac{L}{4\sqrt{6}}, \tag{4.17}$$

which is also a constant. We have the efficiency

$$\eta = \frac{Q + Q^{2/3}(Q - L)^{1/3} + Q^{1/3}(Q - L)^{2/3} - L}{Q + 15Q^{2/3}(Q - L)^{1/3} + 3Q^{1/3}(Q - L)^{2/3} - 3L}, \tag{4.18}$$

and the Carnot efficiency is

$$\eta_c = \frac{19L - 6L(1 - L/Q)^{1/3} - 21Q + 6Q^{2/3}(Q - L)^{1/3} + 12Q^{1/3}(Q - L)^{2/3}}{19(L - Q)} \tag{4.19}$$

This result is interesting since both  $\eta$  and  $\eta_c$  are independent of the normalization factor  $a$  and only depend on the constant  $L$  and charge  $Q$ , implying that the effects of the quintessence field on the efficiency of the heat engine can be eliminated by employing the thermodynamical quantities listed in Eqs. (4.15) and (4.16). It is not hard to check that the efficiencies  $\eta$  and  $\eta_c$  we calculate here are equivalent to the efficiency calculated for pure RN-AdS black holes as discussed in Ref. [61]. We have expansions of the efficiencies at large  $Q$  of

$$\eta = \frac{3}{19} - \frac{8L}{361Q} - \frac{416L^2}{61,731Q^2} - \frac{3286L^3}{1,172,889Q^3} + \mathcal{O}(Q^{-4}) \tag{4.20}$$

and

$$\eta_c = \frac{3}{19} + \frac{8L^3}{513Q^3} + \frac{14L^4}{513Q^4} + \mathcal{O}(Q^{-5}). \tag{4.21}$$

These two expansions coincide with the results shown in Ref. [61] and indicate that the efficiency  $\eta$  will approach the Carnot limit when charge  $Q$  goes to infinity and Fig. 16 is plotted to show the behavior of  $\eta$ ,  $\eta_c$  and the ratio  $\eta/\eta_c$  under the change of  $Q$ . This model also reflects the fact that the choices of the thermodynamical quantities used to construct the heat engine is essential and crucial for the property of the heat engine as we find in this section that the engine efficiency does not depend on the quintessence field which plays a role in influencing the efficiency for the engine discussed previously in this paper.

### 5 Conclusions and discussions

In this paper, we study the heat engine where the charged AdS black hole surrounded by dark energy is the working substance and the mechanical work is done via the  $PdV$  term of the first law of black hole thermodynamics in the extended phase space. We first investigate the effects of a kind of dark energy (quintessence field in this paper) on the efficiency of the RN-AdS black holes as heat engine defined as a rectangle closed path in the  $P-V$  plane. We find that the quintessence field can improve the heat engine efficiency, which will increase as the field density  $\rho_q$  grows. Under some fixed parameters, we find that bigger volume difference between the smaller black holes ( $V_1$ ) and the bigger black

holes ( $V_2$ ) will lead to a lower efficiency, and the bigger pressure difference will make the efficiency higher but the efficiency is always smaller than 1 and will never be larger than the Carnot heat engine; this is consistent with the heat engine in traditional thermodynamics. As the pressure difference  $P_1 - P_4$  goes to infinity, the efficiency will approach the value 1 and meanwhile will also approach the Carnot limit, which is the maximum value of the heat engine efficiency allowed by thermodynamical laws. We find that for some large normalization factor  $a$  (or large quintessence field density  $\rho_q$ ) and electric charge  $Q$  can make some thermodynamical quantities unphysical and subsequently these unphysical quantities lead to the efficiency  $\eta > 1$  and  $\eta > \eta_c$ , which is not permitted by the laws of nature, and to avoid this problem both the factors  $a$  and  $Q$  may should be restricted to a certain range. We discuss the efficiency under the change of the state parameter  $\omega_q$ . With the help of Fig. 10, we find that with the increase of  $\omega_q$  ( $-1 \rightarrow 0$ ) the efficiency decreases monotonously. For  $\eta/\eta_c$ , it will decrease first and then increase with growing  $\omega_q$ , and the bigger  $a$  corresponds to a bigger value of  $\eta/\eta_c$  at the beginning, while for  $\omega_q$  beyond a certain value (about  $-0.462945$ ), the result is contrary. Finally, inspired by Johnson's latest work [61], we find that the factor  $a$  and electric charge  $Q$  need not to be restricted if we put the thermodynamics cycle in a proper position (near the critical point) in the  $P$ - $V$  plane by using the critical thermodynamical quantities calculated when the state parameter  $\omega_q = -1$ . With this method, we build two different heat engine models by making two different choices of the thermodynamical quantities near the critical point. In model 1, the work done by the heat engine determined by Eqs. (4.1) and (4.2) is not fixed. The efficiencies  $\eta$  and  $\eta/\eta_c$  would increase with the growth of both the charge  $Q$  and  $a$  and the heat engine will approach the Carnot limit when  $a$  or  $Q$  goes to infinity. When  $a = 0$ , we find that the efficiency is independent of the charge  $Q$  and only dependent on the constant ratio  $\alpha$  between  $V_1$  and  $V_2$ . In model 2, we make the work a constant and find that the efficiency is independent of the quintessence field; in other words, the quintessence cannot impact the efficiency of the heat engine provided it is constructed by the choices of Eqs. (4.15) and (4.16). The efficiency will also approach the Carnot limit when  $Q$  goes to infinity as heat engine model 1 does. The different characteristics between the two models also reflect the importance of the choice of the thermodynamical cycle to the property of the heat engines.

This paper have showed the impact of dark energy on the efficiency of four dimensional static charged AdS black holes as heat engines, and it would be of great interest to extend our present investigation to black holes in higher dimensions, and rotating black holes are also very worthwhile to investigate in the quintessence AdS black hole spacetime. It is worth noting that the dual field theoretical interpretation about the quintessence is still unclear, although some attention [57–

59] has been paid to the holographic understanding in the framework of the quintessence dark energy. These problems and our results (especially we find that the quintessence dark energy can improve the efficiency of the holographic heat engines) are meaningful, since they may help us promote our understanding of black hole thermodynamics and the dual field theoretical interpretation of quintessence dark energy, further disclosing the relationship between dark energy and black holes. We leave these problems for future work.

**Acknowledgements** This project is partially supported by NSFC. Hang Liu would like to express gratitude to Yan-Fei Tian for her great help in the process of getting this work finished.

**Open Access** This article is distributed under the terms of the Creative Commons Attribution 4.0 International License (<http://creativecommons.org/licenses/by/4.0/>), which permits unrestricted use, distribution, and reproduction in any medium, provided you give appropriate credit to the original author(s) and the source, provide a link to the Creative Commons license, and indicate if changes were made. Funded by SCOAP<sup>3</sup>.

## References

1. S. Hawking, D.N. Page, Thermodynamics of black holes in anti-De Sitter space. *Commun. Math. Phys.* **87**, 577 (1983)
2. D. Kubiznak, R.B. Mann,  $P$ - $V$  criticality of charged AdS black holes. *JHEP* **1207**, 033 (2012)
3. J. Xu, L.-M. Cao, Y.-P. Hu,  $P$ - $V$  criticality in the extended phase space of black holes in massive gravity. *Phys. Rev. D* **91**, 124033 (2015)
4. R.-G. Cai, L.-M. Cao, L. Li, R.-Q. Yang,  $P$ - $V$  criticality in the extended phase space of Gauss-Bonnet black holes in ads space. *JHEP* **2013**, 1–22 (2013)
5. R. Banerjee, D. Roychowdhury, Critical behavior of Born-Infeld ads black holes in higher dimensions. *Phys. Rev. D* **85**, 104043 (2012)
6. R. Banerjee, D. Roychowdhury, Critical phenomena in Born-Infeld ads black holes. *Phys. Rev. D* **85**, 044040 (2012)
7. H. Liu, X.-H. Meng,  $P$ - $V$  criticality in the extended phase space of charged accelerating ads black holes. *Mod. Phys. Lett. A* **31**, 1650199 (2016). doi:10.1142/S0217732316501996
8. S. Gunasekaran, D. Kubizňák, R.B. Mann, Extended phase space thermodynamics for charged and rotating black holes and Born-Infeld vacuum polarization. *J. High Energy Phys.* **2012**, 1–43 (2012)
9. S.H. Hendi, R.M. Tad, Z. Armanfard, M.S. Talezadeh, Extended phase space thermodynamics and  $p$ - $v$  criticality: Brans-Dicke-Born-Infeld vs Einstein-Born-Infeld-dilaton black holes. *Eur. Phys. J. C* **76**, 1–15 (2016)
10. D.-C. Zou, S.-J. Zhang, B. Wang, Critical behavior of Born-Infeld ads black holes in the extended phase space thermodynamics. *Phys. Rev. D* **89**, 044002 (2014)
11. D.-C. Zou, Y. Liu, B. Wang, Critical behavior of charged Gauss-Bonnet-ads black holes in the grand canonical ensemble. *Phys. Rev. D* **90**, 044063 (2014)
12. B. Mirza, Z. Sherkatghanad, Phase transitions of hairy black holes in massive gravity and thermodynamic behavior of charged ads black holes in an extended phase space. *Phys. Rev. D* **90**, 084006 (2014)

13. D. Kastor, S. Ray, J. Traschen, Enthalpy and the mechanics of ads black holes. *Class. Quantum Gravity* **26**, 195011 (2009)
14. B. Dolan, The cosmological constant and the black hole equation of state. *Class. Quantum Gravity* **28**, 125020 (2011)
15. B. Dolan, Pressure and volume in the first law of black hole thermodynamics. *Class. Quantum Gravity* **28**, 235017 (2011)
16. B. Dolan, Compressibility of rotating black holes. *Phys. Rev. D* **84**, 127503 (2011)
17. M. Cvetič, G. Gibbons, D. Kubiznak, C. Pope, Black hole enthalpy and an entropy inequality for the thermodynamic volume. *Phys. Rev. D* **84**, 024037 (2011)
18. A. Belhaj, M. Chabab, H.E. Moumni, M. Sedra, On thermodynamics of ads black holes in arbitrary dimensions. *Chin. Phys. Lett.* **29**, 100401 (2012)
19. S. Hendi, M. Vahidinia, Extended phase space thermodynamics and  $p$ - $v$  criticality of black holes with nonlinear source. *Phys. Rev. D* **88**, 084045 (2013)
20. E. Spallucci, A. Smailagic, Maxwells equal area law for charged anti-de Sitter black holes. *Phys. Lett. B* **723**, 436–441 (2013)
21. N. Altamirano, D. Kubiznak, R. Mann, Z. Sherkatghanad, Thermodynamics of rotating black holes and black rings: phase transitions and thermodynamic volume. *Galaxies* **2**, 89–159 (2014)
22. S.H. Hendi, R.B. Mann, S. Panahiyan, B.E. Panah, van der waals like behaviour of topological ads black holes in massive gravity. *Phys. Rev. D* **95**, 021501 (2017)
23. S.H. Hendi, G.-Q. Li, J.-X. Mo, S. Panahiyan, B.E. Panah, New perspective for black hole thermodynamics in Gauss–Bonnet–Born–Infeld massive gravity. *Eur. Phys. J. C* **76**, 571 (2016)
24. S.H. Hendi, S. Panahiyan, B.E. Panah, M. Faizal, M. Momennia, Critical behavior of charged black holes in Gauss–Bonnet gravity’s rainbow. *Phys. Rev. D* **94**, 024028 (2016)
25. S.H. Hendi, S. Panahiyan, B.E. Panah, Extended phase space of black holes in loveclock gravity with nonlinear electrodynamics. *Prog. Theor. Exp. Phys.* **2015**, 103E01 (2015)
26. C.V. Johnson, Holographic heat engines. *Class. Quantum Gravity* **31**, 205002 (2014)
27. J.-X. Mo, F. Liang, G.-Q. Li, Heat engine in the three-dimensional spacetime. *J. High Energy Phys.* **2017**, 10 (2017)
28. C.V. Johnson, Gauss–Bonnet black holes and holographic heat engines beyond large  $n$ . *Class. Quantum Gravity* **33**, 215009 (2016)
29. C.V. Johnson, Born–Infeld ads black holes as heat engines. *Class. Quantum Gravity* **33**, 135001 (2016)
30. A. Belhaj, M. Chabab, H.E. Moumni, K. Masmarr, M.B. Sedra, A. Segui, On heat properties of ads black holes in higher dimensions. *JHEP* **05**, 149 (2015)
31. M.R. Setare, H. Adami, Polytrropic black hole as a heat engine. *Gen. Relativ. Grav.* **47**, 133 (2015)
32. E. Caceres, P.H. Nguyen, J.F. Pedraza, Holographic entanglement entropy and the extended phase structure of STU black holes. *JHEP* **1509**, 184 (2015)
33. C.V. Johnson, An exact efficiency formula for holographic heat engines. *Entropy* **18**, 120 (2016)
34. S.W. Wei, Y.X. Liu, Implementing black hole as efficient power plant. [arXiv:1605.04629](https://arxiv.org/abs/1605.04629) (2016)
35. M. Zhang, W.-B. Liu,  $f(r)$  black holes as heat engines. *Int. J. Theor. Phys.* **55**, 5136–5145 (2016)
36. J. Sadeghi, K. Jafarzade, Heat engine of black holes. [arXiv:1504.07744](https://arxiv.org/abs/1504.07744)
37. J. Sadeghi, K. Jafarzade, The correction of Horava–Lifshitz black hole from holographic engine. [arXiv:1604.02973](https://arxiv.org/abs/1604.02973)
38. C. Bhamidipati, P.K. Yerra, Heat engines for dilatonic Born–Infeld black holes. [arXiv:1606.03223](https://arxiv.org/abs/1606.03223)
39. R.A. Hennigar, F. McCarthy, A. Ballon, R.B. Mann, Holographic heat engines: general considerations and rotating black holes. [arXiv:1704.02314](https://arxiv.org/abs/1704.02314) [hep-th]
40. S.H. Hendi, B.E. Panah, S. Panahiyan, H. Liu, X.-H. Meng, Black holes in massive gravity as heat engines. [arXiv:1707.02231](https://arxiv.org/abs/1707.02231) [hep-th]
41. J.-X. Mo, G.-Q. Li, Holographic heat engine within the framework of massive gravity. [arXiv:1707.01235](https://arxiv.org/abs/1707.01235) [gr-qc]
42. N. Bachall, J. Ostriker, S. Perlmutter, P. Steinhardt, The cosmic triangle: revealing the state of the universe. *Science* **284**, 1481 (1999)
43. S. Perlmutter et al., Measurements of  $\Omega$  and  $\Lambda$ -term from high-redshift supernovae. *Astrophys. J.* **517**, 565 (1999)
44. V. Sahni, A. Starobinsky, The case for a positive cosmological  $\lambda$ -term. *Int. J. Mod. Phys. D* **9**, 373 (2000)
45. Y. Fujii, Origin of the gravitational constant and particle masses in a scale-invariant scalar-tensor theory. *Phys. Rev. D* **26**, 2580 (1982)
46. L. Ford, Cosmological constant damping by unstable scalar fields. *Phys. Rev. D* **35**, 2339 (1987)
47. B. Ratra, P. Peebles, Cosmological consequences of a rolling homogeneous scalar field. *Phys. Rev. D* **37**, 3406 (1988)
48. C. Wetterich, Cosmology and the fate of dilatation symmetry. *Nucl. Phys. B* **302**, 668 (1988)
49. V. Kiselev, Quintessence and black holes. *Class. Quantum Gravity* **20**, 1187–1198 (2003)
50. S. Chen, J. Jing, Quasinormal modes of a black hole surrounded by quintessence. *Class. Quantum Gravity* **22**, 4651–4657 (2005)
51. S. Chen, B. Wang, R. Su, Hawking radiation in a  $d$ -dimensional static spherically symmetric black hole surrounded by quintessence. *Phys. Rev. D* **77**, 124011 (2008)
52. N. Varghese, V. Kuriakose, Massive charged scalar quasinormal modes of reissner-nordstrom black hole surrounded by quintessence. *Gen. Relativ. Grav.* **41**, 1249–1257 (2009)
53. R. Tharanath, V. Kuriakose, Phase transition, quasinormal modes and Hawking radiation of Schwarzschild black hole in quintessence field. *Mod. Phys. Lett. A* **29**, 1450057 (2014)
54. M. Ainou, M. Rodrigues, Geometrical and Poincaré methods for charged black holes in presence of quintessence. *J. High Energy Phys.* **1309**, 146 (2013)
55. Y. Wei, Z. Chu, Thermodynamic properties of a Reissner–Nordstrom quintessence black hole. *Chin. Phys. Lett.* **28**, 100403 (2011)
56. M. Saleh, B. Bouetou, T. Kofane, Quasinormal modes of gravitational perturbation around a Reissner–Nordstrom black hole surrounded by quintessence. *Chin. Phys. Lett.* **26**, 109802 (2009)
57. X.-X. Zeng, D.-Y. Chen, L.-F. Li, Holographic thermalization and gravitational collapse in a spacetime dominated by quintessence dark energy. *Phys. Rev. D* **91**, 046005 (2015)
58. X.-X. Zeng, L.-F. Li, Van der waals phase transition in the framework of holography. *Phys. Lett. B* **764**, 100–108 (2017)
59. S. Chen, Q. Pan, J. Jing, Holographic superconductors in quintessence ads black hole. *Class. Quantum Gravity* **30**, 145001 (2013)
60. G.-Q. Li, Effects of dark energy on pvcriticality of charged ads black holes. *Phys. Lett. B* **735**, 256–260 (2014)
61. C. V. Johnson, Approaching the Carnot limit at finite power: an exact solution. [arXiv:1703.06119](https://arxiv.org/abs/1703.06119)